MicroRNAs accurately identify cancer tissue origin

Nitzan Rosenfeld[1,8], Ranit Aharonov[1,8,†], Eti Meiri[1,8], Shai Rosenwald[1,8], Yael Spector[1], Merav Zepeniuk[1], Hila Benjamin[1], Norberto Shabes[1], Sarit Tabak[1], Asaf Levy[1], Danit Lebanony[1], Yaron Goren[1], Erez Silberschein[1,‡], Nurit Targan[1], Alex Ben-Ari[1], Shlomit Gilad[1], Netta Sion-Vardy[2], Ana Tobar[3], Meora Feinmesser[3] , Oleg Kharenko[4], Ofer Nativ[5], Dvora Nass[6,7], Marina Perelman[6,7], Ady Yosepovich[6,7], Bruria Shalmon[6,7], Sylvie Polak-Charcon[6,7], Eddie Fridman[6,7], Amir Avniel[1], Isaac Bentwich[1], Zvi Bentwich[1], Dalia Cohen[1], Ayelet Chajut[1] & Iris Barshack[6,7,†]

[1]Rosetta Genomics Ltd., Rehovot, 76706, Israel. [2]Soroka University Medical Center, Beer-Sheva, 84101, Israel. [3]Department of Pathology, Beilinson hospital, Rabin Medical Center, Petah-Tikva, 49100, Israel. [4]Pathology Institute, Sourasky Medical Center, Tel Aviv, 64239, Israel. [5]Bnai-Zion Medical Center, Haifa, 31048, Israel. [6]Department of Pathology, Sheba Medical Center, Tel-Hashomer, 52621, Israel. [7]Sackler School of Medicine, Tel-Aviv University, Tel-Aviv, Israel.

[8]N.R., R.A., E.M. and S.R. contributed equally to this work.

[‡]E.S. was engaged as an external consultant to Rosetta Genomics.

[†]Correspondence should be addresses to

R.A. (ranit_ah@rosettagenomics.com) or I.B. (barshack@sheba.health.gov.il)

Nature Biotechnology 2008 - Supplementary Information (available online)

This supplementary file includes:

Supplementary Figures 1-7 and Supplementary Table 4.

<u>Additional Supplementary Tables are available online as excel spreadsheets:</u>

Supplementary Table 1: Details of samples and microRNA expression levels.

Supplementary Table 2: Parameters of the logistic regression classifier at each node.

Supplementary Table 3: Performance of the classifiers on the training set and on the blinded test set.

Supplementary Table 5: Validation by qRT-PCR.

Supplementary Figures

Supplementary Fig. 1: Comparison of microRNA profiles of RNA extracted from fresh-frozen, formalin-fixed, and FFPE samples.

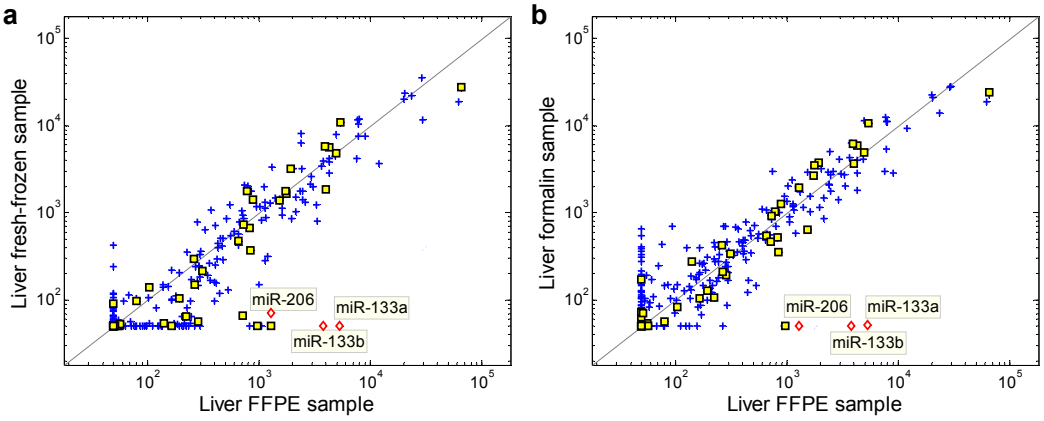

a) RNA was extracted and profiled (4 µg total RNA) from a mouse liver sample which was either preserved as fresh-frozen (y-axis) or FFPE (x-axis). Yellow squares show the 48 microRNAs used in the decision-tree (Table 2, Table S2). Overall correlation of expressions was 0.9, for all the microRNAs and for the subset of 48 microRNAs. Strong outliers are muscle-specific microRNAs, ostensibly due to neighboring muscle tissue in the FFPE sample. Similar results were obtained for RNA extracted from lung.

b) Similar results were obtained when comparing microRNA expression extracted from FFPE sample (x-axis) to the RNA extracted from formalin-fixed sample (y-axis). Overall correlation of expressions was 0.9, for all the microRNAs and for the subset of 48 microRNAs. Similar results were obtained for RNA extracted from lung.

We next examined the difference in the level of microRNA expression in tissues (liver & lung) preserved at different time points, immediate, 1h & 5h post operation. The microRNA fraction in the lung was not affected even when kept non-fixed for 5 hours. Delaying fixation of a liver sample by 1 hour had no significant change on the microRNA fraction, but the microRNA fraction was decreased approximately 2-fold when the liver sample was kept non-fixed for 5 hours, reflecting the high content of nucleases in liver tissue (data not shown).

Supplementary Fig. 2: Stability of microRNA profile in FFPE samples for as long as 11 years of storage.

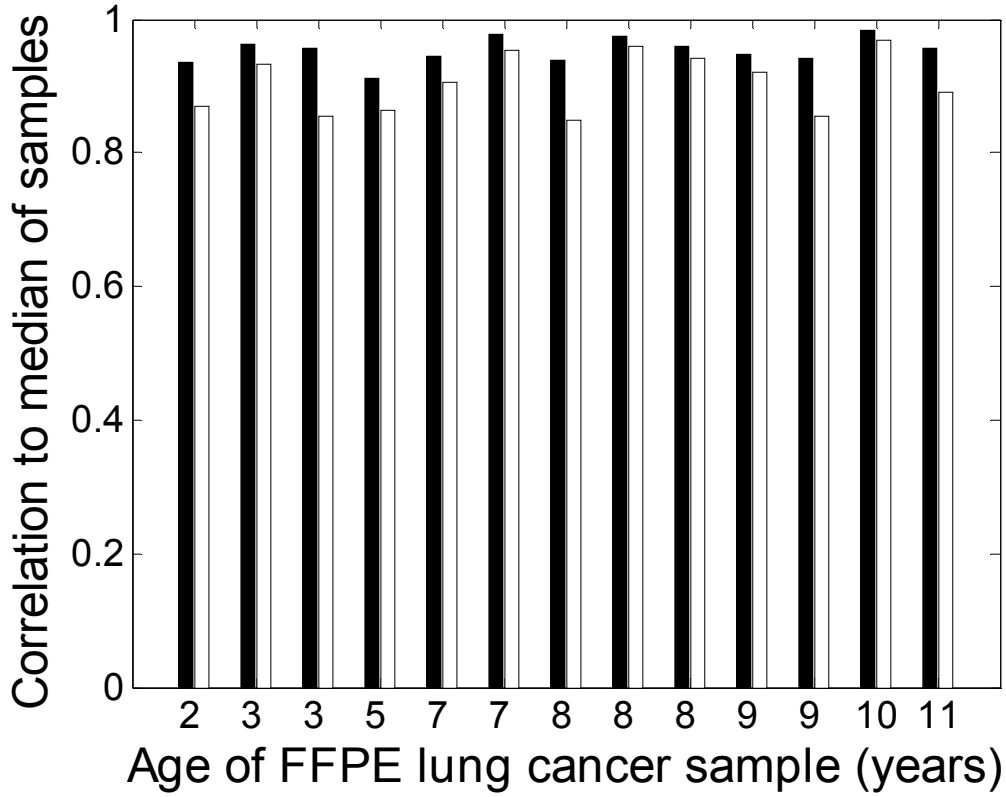

Total RNA was extracted from 13 lung cancer FFPE samples of different ages (ages 2-11 years) and hybridized to the miRdicator™ microarray. Each full bar in the graph depicts the overall microRNA expression correlation (Pearson correlation coefficient) between a single sample (age appearing on the x-axis), and the median of all samples. The high correlation (mostly above 0.9) indicates the highly preserved fraction of microRNA in paraffin blocks even after many years. Empty bars show the correlation for the 48 microRNAs used in the decision-tree (Table 2, Table S2), which reach 0.9 on average.

Supplementary Fig. 3: Reproducibility, sensitivity and specificity of microRNA microarray platform

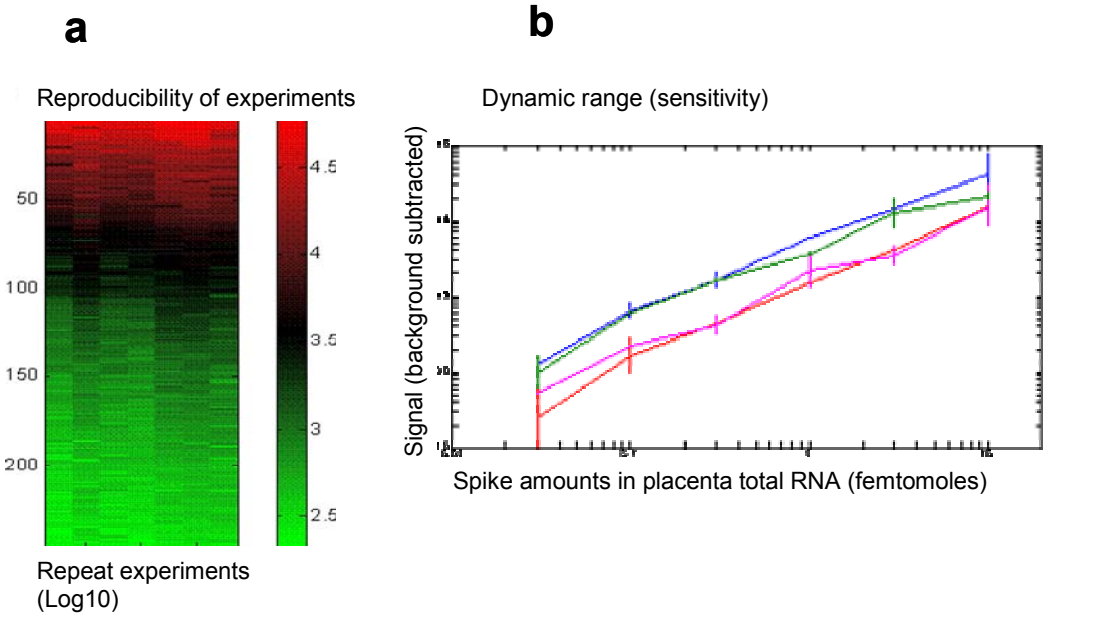

c

Specificity

	let-7a	let-7c	let-7d
let-7a	100	10	2
let-7c	10	100	3
let-7d	9	3	100
let-7b	7	8	4
let-7e	2	1	1
let-7f	3	1	0
let-7g	1	1	0
let-7i	2	1	1

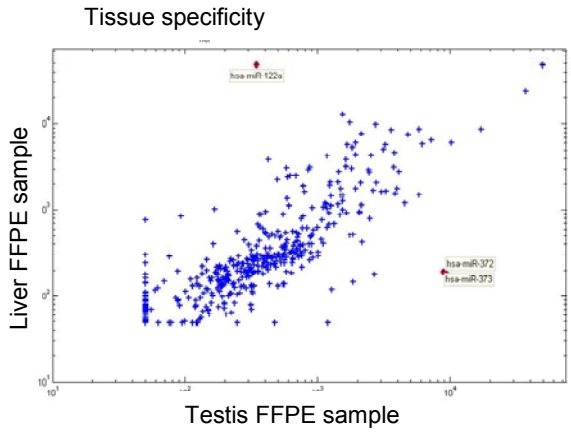

a) Microarray reproducibility: 3 µg of placenta RNA (Ambion) was repeatedly (seven times) labeled and hybridized to the microarray. For >200 highly expressed microRNAs (sorted from top to bottom by mean expression level), each column depicts the expression in one repeat. For each pair of repeats the Pearson correlation coefficient was computed resulting in an overall mean correlation coefficient of 0.99.

b) Microarray sensitivity & dynamic range: four synthetic short RNAs, 22 nt long, were spiked in different amounts into 3 μg of placenta total RNA, labeled and hybridized to the array. Each line corresponds to one of the spike-ins. The lowest sensitivity was found to be 0.1 fmole with a linear dynamic range of about three orders of magnitude.

c) Microarray specificity: synthetic RNAs of hsa-let-7a, c & d were spiked into non-relevant background material (high molecular weight RNA extracted from HeLa cell line, which shows no hybridization background when hybridized to the microarray, data not shown) and hybridized to the miRdicator^{TM} microarray. The table depicts the probe signals of the let-7 family in response to the spiked-in synthetic RNAs (columns), normalized by the signal of the probe corresponding to the synthetic RNA. Specificity of about 10-fold in the signal level between let-7a and let-7c was demonstrated, representing the level of specificity for a single nucleotide mismatch.

d) Tissue specificity: 3-5 μg of total RNA extracted from liver and testis FFPE samples were labeled and hybridized to the miRdicator^{TM} microarray, identifying tissue specific microRNA expression profiles such as hsa-miR-122a in the liver and hsa-miR-372 and hsa-miR-373 in the testis tissue.

Supplementary Fig. 4: Comparison of microRNA expression in primary and metastatic tumor samples.

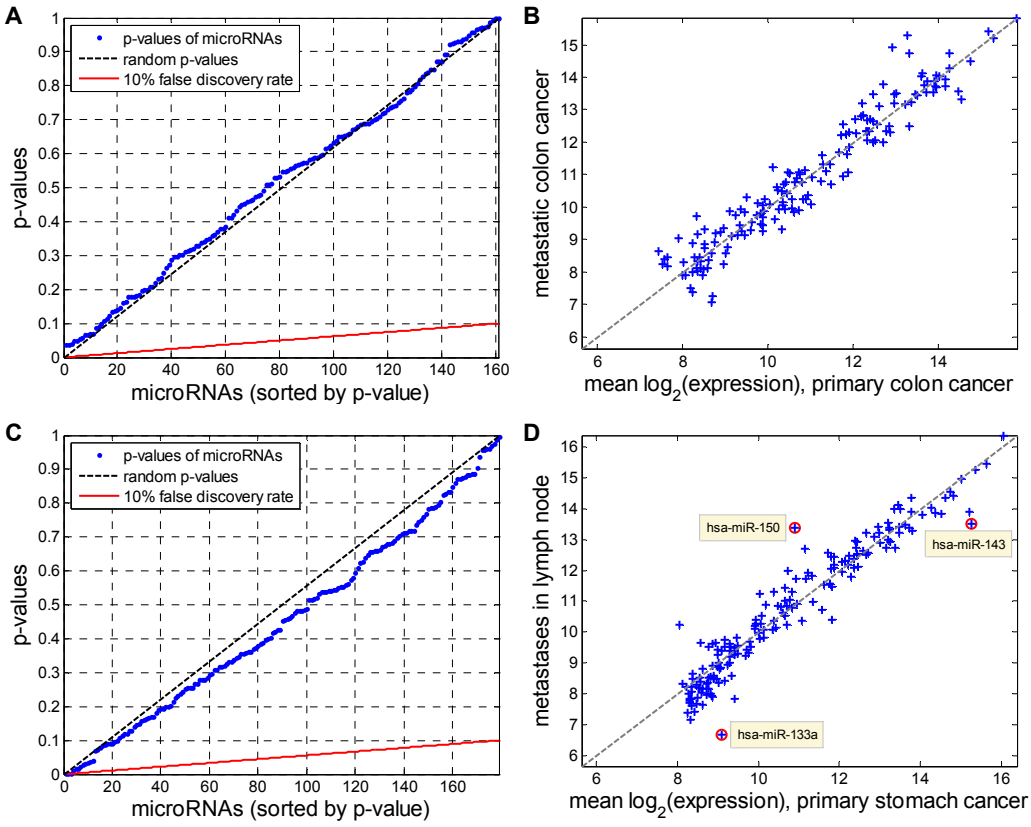

A) Primary and metastatic colon cancer samples were compared, and p-values (unpaired t-test on the log-signal) were calculated for each microRNA that passes a signal threshold in at least one of the sets. The sorted p-values (blue dots) agreed with a random distribution of p-values (uniform in the range 0-1, dotted black line). The red line indicates the 10% false discovery rate (FDR) line – p-values below this line have a 10% probability of false discovery. For colon cancer metastases, none of the features passed a 10% false-discovery test. Similarly, in comparison between breast cancer cases that were positive or negative for ER-PR or for Her2/neu, no microRNAs were found to have statistically significant differences in expression levels.

B) Dot-plot of the mean $\log_2$ signals of the primary vs. the metastatic colon cancer samples (blue crosses; dotted black line is a guide to the eye showing diagonal where mean expression is equal).

C) Comparison (as in A) of primary stomach cancers to stomach cancer metastases to the lymph nodes. The first three microRNAs with lowest p-values passed the false discovery test (at 10% false discovery rate).

D) Dot-plot (as in B) of the primary stomach cancers vs. stomach metastases to the lymph node. The three microRNAs that passed the FDR test are highlighted: miR-133a and miR-143 were over-expressed in the primary tumors, miR-150 was over-expressed in the metastases.

Supplementary Fig. 5: An automatically generated tree using a CART algorithm.

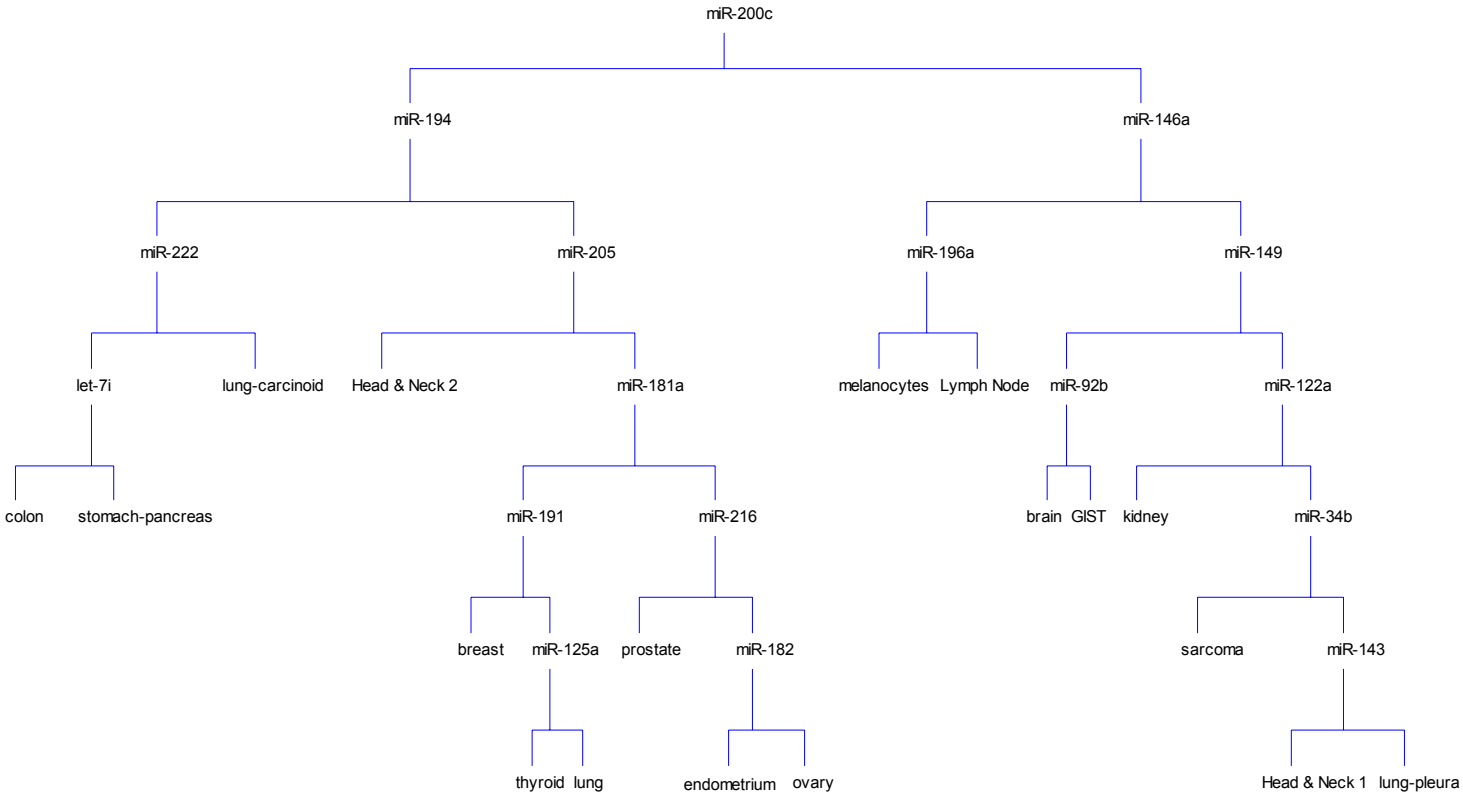

The "Classification And Regression Tree" (CART) method (see e.g. Allory et al., Histopathology 2008, 52:158-166 for an application in pathology) generates locally-optimized binary trees for classification, finding at each step a data feature (microRNA expression level) that divides the data into two groups. Classes are grouped together based on the ability to distinguish between them using a single feature (or a combination of several features, in the decision-tree in Fig. 1) and not on the basis of overall similarity (such as by correlation). Some classes fail to be separated (e.g. the "stomach-pancreas" leaf), whereas other classes may be split between two branches (e.g. the "Head & Neck 1" and "Head & Neck 2" leaves). Here only classes with more than 3 representative samples in the training set were used. The overall structure is highly similar to the one obtained by a more biologically-driven approach (Fig. 1). At each node only one data feature is used (indicated at the node). The overall performance was significantly poorer than other algorithms, reaching less than 50% accuracy in the test set.

Supplementary Fig. 6: A logistic regression model in one dimension.

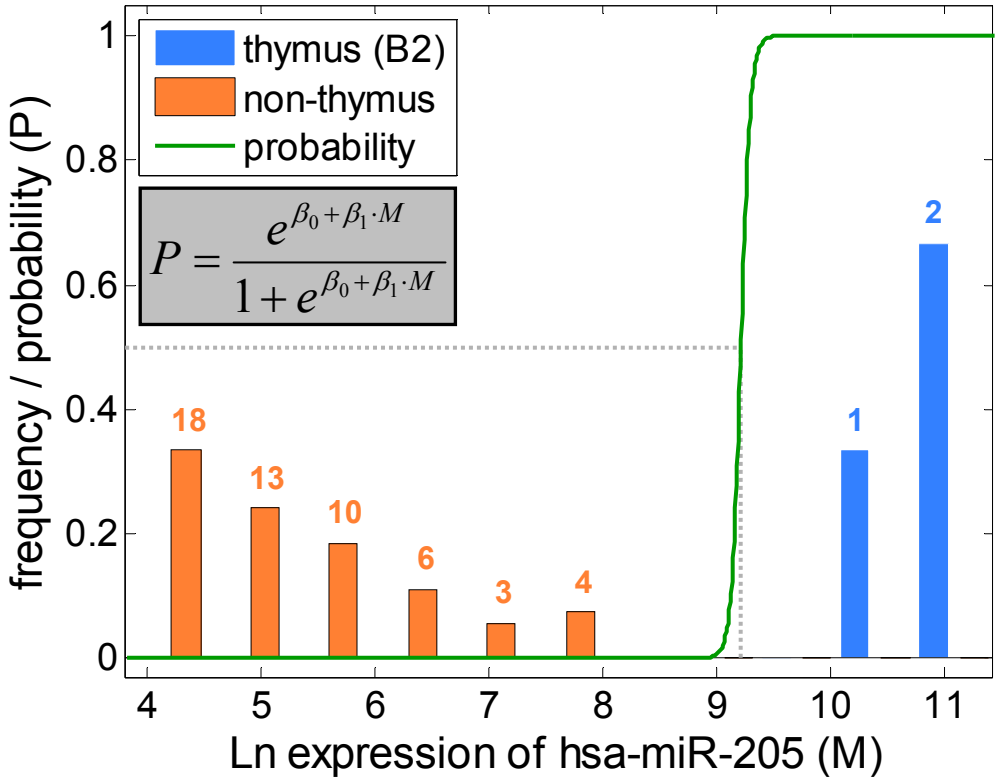

The logistic regression model for node #8 in the tree (Methods, Table S2) assigns each sample a probability (P, solid curve) of belonging to the group in the left branch (i.e. thymus B2) as a function (inset) of the expression level of hsa-miR-205 in the sample (M is the natural log of the measured expression level). Bars show the distribution of the expression levels of hsa-miR-205 in thymus B2 samples (left in node #8, blue) and samples (right in node #8, orange). Numbers indicate the number of samples in each bin. Samples with M>9.2 have P>0.5 (dotted grey lines) and are assigned to the thymus class, whereas all other samples are assigned to the right branch at node #8 and continue with classification by other decision nodes.

Supplementary Fig. 7: Accuracy of classification using the qRT-PCR data.

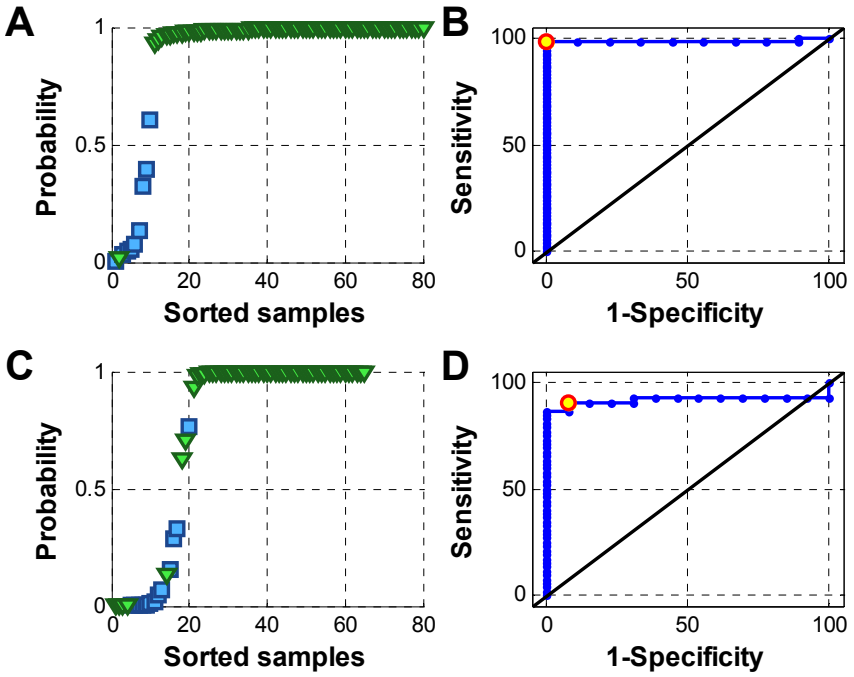

The receiver operating characteristic curve (ROC curve) plots the sensitivity against the false-positive rate (one minus the specificity) for different cutoff values of a diagnostic metric, and is a measure of classification performance. The area under the ROC curve (AUC) can be used to assess the diagnostic performance of the metric. A random classifier has AUC=0.5, and an optimal classifier with perfect sensitivity and specificity of 100% has AUC=1.

A) Probability (P) output of a logistic classifier trained to separate liver from non-liver samples using the expression levels of hsa-miR-122a and hsa-miR-141 measured in qRT-PCR (Fig 2C). Blue squares show the 9 liver samples, green triangles show the 71 non-liver samples. A threshold at P_{th}=0.8 easily separates the two classes, with one outlier.

B) The corresponding ROC curve has AUC=0.988, near the optimum. Red circle shows P_{th}=0.8 which has 100% sensitivity and 99% specificity in identifying liver samples.

C) Probability (P) output of a logistic classifier trained to separate gastrointestinal (GI) samples from non-GI samples using the expression levels of hsa-miR-145, hsa-miR194 and hsa-miR-205 (at node #12 in the decision-tree, Fig. 1) measured in qRT-PCR (Fig 2D). Blue squares show the 13 colon or pancreas samples, green triangles show the 52 other epithelial samples (right branch at node #12). A threshold at P_{th}=0.5 has 6 errors.

D) The corresponding ROC curve has AUC=0.914. Red circle shows P_{th}=0.5, which has 92% sensitivity and 91% specificity in identifying the gastrointestinal samples. Using the parameters of the logistic regression that was trained for the microarray data (Table S2) results in sensitivity of 93% and specificity of 97% for the microarray data (Fig. 2B) and specificity of 92% and sensitivity of 92% for the transformed qRT-PCR data (Fig. 2D).

Supplementary Table 4: Information on the microRNAs used for classification.
(References for Table 4 are listed below)

microRNA name	**Appears in node(s)** (R) means microRNA expression is higher in right branch, (L) means higher in left branch.	**Information**
hsa-let-7e	13(R)	High expression in normal ovary and skeleton muscle compared to other normal tissues[1].
hsa-let-7i	14(R), 15(R), 17(L), 19(L)	Regulates TLR4 expression in cholangiocytes and contributes to epithelial immune responses against C. parvum infection[2].
hsa-miR-9*	6(L)	Found in brain tumors and derived cell-lines[3] and was found to be expressed specifically in the developing nervous system[4-7].
hsa-miR-10b	20(R)	Highly expressed in metastatic breast cancer cells and positively regulates cell migration and invasion [8]. Highly expressed in normal ovary, compared to other normal tissues[1].
hsa-miR-19b	15(L)	High expression in Hela S3 compared to normal tissues[1].
hsa-miR-21	9(R), 13(L)	Regulates expression of the PTEN tumor suppressor gene in human hepatocellular cancer[9].
hsa-miR-27b	17(R)	Expression of miR-27b contributes to in vitro angiogenesis[10].
hsa-miR-29a	14(L)	One of the human microRNAs which target the nef gene in HIV-1 as evidenced by computational predictions[11].
hsa-miR-29b	11(R)	Predominantly localized to the nucleus; the hexanucleotide terminal motif of miR-29b acts as a transferable nuclear localization element that directs nuclear enrichment of miRNAs or small interfering RNAs to which it is attached[12].
hsa-miR-29c	22(L)	High expression in chronic lymphocytic leukemias (CLL)[13].
hsa-miR-31	16(R)	high expression in normal colon compared to other normal tissues[1].
hsa-miR-34a	24(L)	Functions as a potential tumor suppressor by inducing apoptosis in neuroblastoma cells (done by repressing translation of E2F3 gene)[14]. Also known to repress translation of DLL1 and Notch1 genes[15]. It is transcriptionally activated by p53 and contributes to p53-mediated apoptosis[16].
hsa-miR-34b	9(R)	The expression of miR-34b is robustly induced by DNA damage and oncogenic stress in a p53-dependent manner[17].
hsa-miR-92	4(L)	The levels of miR-92 (together with miR-19) rise as a response to over-expression of pri-miR-106-363, as observed in 46% of human T-cells leukemias[18]. A part of a known oncogenic miRNA cluster (cluster 17-92), that was also shown to be upregulated in response to a potent hepatocarcinogen in rats[19].
hsa-miR-92b	6(L)	Found in brain tumors and derived cell lines[3], and was found to be expressed specifically in the developing nervous system[4-7].
hsa-miR-99a	20(R)	Up-regulated in acute megakaryoblastic cell lines compared with *in vitro*-differentiated megakaryocytes[20]. Expression profile in normal tissues[1,21] fully support higher expression of miR-99a in hormonal reproductive tissues (ovary, uterus, cervix, prostate, breast) than in non-hormonal tissues (bladder, lung). Located in a region of 2.84Mb in 21q11.1 which was found to be deleted in lung cancers[22].

hsa-miR-106b	19(R)	Two sequence alterations, in hepatocellular carcinoma (HCC) tissues and liver cancer derived cell lines, were located in miR-106b and identified as known single nucleotide polymorphisms[23]
hsa-miR-122a	1(L)	Found to be liver-specific in normal human tissue expression profiles. Represses translation of CAT-1 gene. Modulates hepatitis C virus RNA abundance[1,21,24-26]
hsa-miR-124	6(L)	Mouse miR-124 dominated and accounted for 25%-48% of all mouse brain miRNAs[24]. mir-124 is highly represented in expression libraries from adult brain tissue and is preferentially expressed in neurons[27]. Found to be brain-specific in normal human tissue expression profiles[1,21]. This microRNA has many validated target genes[27-30]. The transcriptional repressor, RE1 silencing transcription factor (REST), has a reciprocal activity, inhibiting the expression of neuronal genes in non-neuronal cells. REST regulates the expression of a family of miRNAs, including brain-specific miR-124[30].
hsa-miR-130a	7(L)	Was up-regulated in hepatomas compared to the livers from age-matched rats on a normal diet[31].
hsa-miR-138	19(L)	Over-expressed in normal brain compared to other normal tissues[1].
hsa-miR-141	18(L)	Lower expression in normal liver than in normal pancreas, small intestine, colon, prostate, breast, lung, and bladder[1]. Represses Translation of Clock gene[32]. Highly over-expressed in malignant cholangiocytes vs. nonmalignant cholangiocytes[33]. Hsa-miR-141 and hsa-miR-200c are part of one predicted polycistronic pri-microRNA[3], in an intronic region of a transcription unit (EST with no ORF) on Chr.12p13.31, and their expression is likely to be co-regulated[1].
hsa-miR-142-3p	5(L)	Over-expressed in leukemia cell lines compared to other human cancer cell lines[34]. Trans-gene expression from vectors incorporating target sequences for mir-142-3p was effectively suppressed in intra-vascular and extra-vascular hematopoietic lineages, whereas expression maintains in non-hematopoietic cells[35].
hsa-miR-145	12(L)	Significantly deregulated in colorectal cancer[36].
hsa-miR-146a	4(R)	Significantly over-expressed in psoriatic lesional skin but not in atopic eczema lesions when compared with healthy skin. CD4+CD25 (high) regulatory T cells, monocyte-derived dendritic cells and mast cells expressed miR-146a at a high level[37].
hsa-miR-148b	24(L)	
hsa-miR-152	7(L), 21(L)	Aberrant hyper-methylation was shown for mir-152 in some cases of primary human breast cancer specimens[38].
hsa-miR-181a	3(R)	Increasing miR-18a expression in mature T cells augments the sensitivity to peptide antigens, while inhibiting miR-18a expression in immature T cells reduces sensitivity and impairs both positive and negative selection. Preferentially expressed in the B-lymphoid cells of bone marrow; its ectopic expression in hematopoietic stem/progenitor cells led to an increased fraction of B-lineage cells in both tissue-culture differentiation assays and adult mice[39,40]
hsa-miR-181b	17(L)	Modulates hematopoietic lineage differentiation[40]. miR-181 and

		miR-29 regulate Tcl1 expression in Chronic Lymphocytic Leukemia[41]. miR-181 targets the homeobox protein Hox-A11 during mammalian myoblast differentiation[42] . Downregulated in glioblastoma[43]. Downregulated in acute promyelocytic leukemia during all-trans-retinoic acid treatment[44]. Higher expression in normal human pancreas and colon than in normal breast, crevix and lung[28]. It is upregulated in breast, prostate, and pancreatic cancers[45].
hsa-miR-182	22(L), 24(L)	Over expressed in normal lung and thymus compared to other normal tissues[46].
hsa-miR-187	11(R)	Over-expressed in melanoma cell lines compared to other tumor cell lines[34].
hsa-miR-192	9(R), 23(L)	A key microRNA highly expressed in the kidney. One of its targets is SIP1 (an E-box repressor). miR-192 levels also were increased by TGF-beta in MMC. miR-192 synergized with deltaEF1 short hairpin RNAs to increase Col1a2 E-box-luc activity[47].
hsa-miR-193a	16(L)	Highly expressed in Breast carcinoma compared to normal and malignant cells and tissues[3]
hsa-miR-193b	18(R)	
hsa-miR-194	10(R), 12(L)	High expression in microarray in colon and small intestine, low expression in prostate, breast, uterus, cervix, lung, bladder[21]. Higher expression of this microRNA in normal human pancreas, small intestine and colon than in breast, prostate, cervix, uterus, lung and bladder[1].
hsa-miR-196a	16(L)	Highly expressed in Breast-adeno-carcinoma compared to other normal and malignant cells and tissues[3]. Over-expressed in breast cancer cell lines compared to other human cancer cell lines[34].
hsa-miR-200a	4(R)	Shown to be significantly over-expressed in human ovarian cancer in comparison to normal ovary[48].
hsa-miR-200c	1(R),3(L)	Significantly over-expressed in breast adenocarcinoma and breast duct carcinoma compared to other malignant and normal cells and tissues. Also, over-expressed in normal thyroid, pancreas and prostate compared to other malignant and normal cells and tissues[3]. Over expression of hsa-miR-200c leads to reduced expression of transcription factor 8 and increased expression of E-cadherin[49]. Hsa-miR-141 and hsa-miR-200c are part of one predicted polycistronic pri-microRNA[3], in an intronic region of a transcription unit (EST with no ORF) on Chr.12p13.31, and their expression is likely to be co-regulated[1].
hsa-miR-205	3(L), 12(R), 8(L), 18(R), 21(R)	Highly expressed in cancer cell-lines originating from larynx[50]. MicroRNA Expression profiles in normal human tissues[1,21] supports higher expression of miR-205 in non-digestive tissues (breast,prostate,cervix,bladder,lung) than in digestive tissues (pancreas, colon, small intestine) and higher expression in cervix then in uterus. Also, public data from Affymetrix Human Exon 1.0 ST array (shown in the UCSC genome browser, "Affymetrix All Exon Chips" track) demonstrate that a probe partially overlapping this microRNA precursor (probe 2377993) has a higher signal in breast and prostate than in pancreas and thyroid.
hsa-miR-210	9(R), 10(R), 16(R)	Over-expressed in integrated HPV-16 cell line[51].

hsa-miR-214	15(R)	High expression in normal ovary compared to other normal tissues[1].
hsa-miR-345	22(L), 23(L)	
hsa-miR-363	16(L)	As a part of mir-106a cistron, plays an important role in T cell tumorigenesis[52].
hsa-miR-372	2(L)	A genetic screen implicates miR-372 and miR-373 as oncogenes in testicular germ cell tumors. These miRNAs neutralize p53-mediated CDK inhibition, possibly through direct inhibition of the expression of the tumor-suppressor LATS2[53].
hsa-miR-373	18(R)	See hsa-miR-372
hsa-miR-375	20(L)	Regulates insulin secretion by targeting Myotrophin[54]. Also known to repress translation of Jak2, C1qbp, Usp1 and Adipor2 genes[27].
hsa-miR-382	10(L)	The 3' ends of HIV-1 messenger RNAs are targeted by a cluster of cellular miRNAs including miR-382, which are enriched in resting CD4+ T cells as compared to activated CD4+ T cells[55].
hsa-miR-509	5(R)	

Supplementary References (for Supplementary Table 4):

1. Baskerville, S. & Bartel, D.P. Microarray profiling of microRNAs reveals frequent coexpression with neighboring miRNAs and host genes. *Rna* 11, 241-7 (2005).
2. Chen XM, S.P., O'Hara SP, LaRusso NF. A cellular micro-RNA, let-7i, regulates Toll-like receptor 4 expression and contributes to cholangiocyte immune responses against Cryptosporidium parvum infection. *J Biol Chem*, 28929-38 (2007).
3. Landgraf, P. et al. A Mammalian microRNA Expression Atlas Based on Small RNA Library Sequencing. *Cell* 129, 1401-14 (2007).
4. Kapsimali, M. et al. MicroRNAs show a wide diversity of expression profiles in the developing and mature central nervous system. *Genome Biol* 8, R173 (2007).
5. Krichevsky, A.M., King, K.S., Donahue, C.P., Khrapko, K. & Kosik, K.S. A microRNA array reveals extensive regulation of microRNAs during brain development. *Rna* 9, 1274-81 (2003).
6. Watanabe, T. et al. Stage-specific expression of microRNAs during Xenopus development. *FEBS Lett* 579, 318-24 (2005).
7. Zhao, J.J. et al. Genome-wide microRNA profiling in human fetal nervous tissues by oligonucleotide microarray. *Childs Nerv Syst* (2006).
8. Ma, L., Teruya-Feldstein, J. & Weinberg, R.A. Tumour invasion and metastasis initiated by microRNA-10b in breast cancer. *Nature* 449, 682-8 (2007).
9. Meng, F. et al. MicroRNA-21 Regulates Expression of the PTEN Tumor Suppressor Gene in Human Hepatocellular Cancer. *Gastroenterology* 133, 647-58 (2007).
10. Kuehbacher A, U.C., Dimmeler S. Targeting microRNA expression to regulate angiogenesis. *Trends Pharmacol Sci.* (2007).
11. Hariharan, M., Scaria, V., Pillai, B. & Brahmachari, S.K. Targets for human encoded microRNAs in HIV genes. *Biochem Biophys Res Commun* 337, 1214-8 (2005).
12. Hwang, H.W., Wentzel, E.A. & Mendell, J.T. A hexanucleotide element directs microRNA nuclear import. *Science* 315, 97-100 (2007).

13. Zanette, D.L. et al. miRNA expression profiles in chronic lymphocytic and acute lymphocytic leukemia. *Braz J Med Biol Res* (2007).
14. Welch, C., Chen, Y. & Stallings, R.L. MicroRNA-34a functions as a potential tumor suppressor by inducing apoptosis in neuroblastoma cells. *Oncogene* (2007).
15. Lewis, B.P., Shih, I.H., Jones-Rhoades, M.W., Bartel, D.P. & Burge, C.B. Prediction of mammalian microRNA targets. *Cell* 115, 787-98 (2003).
16. Raver-Shapira, N. et al. Transcriptional activation of miR-34a contributes to p53-mediated apoptosis. *Mol Cell* 26, 731-43 (2007).
17. He, X., He, L. & Hannon, G.J. The guardian's little helper: microRNAs in the p53 tumor suppressor network. *Cancer Res* 67, 11099-101 (2007).
18. Landais, S., Landry, S., Legault, P. & Rassart, E. Oncogenic potential of the miR-106-363 cluster and its implication in human T-cell leukemia. *Cancer Res* 67, 5699-707 (2007).
19. Pogribny, I.P. et al. Induction of microRNAome deregulation in rat liver by long-term tamoxifen exposure. *Mutat Res* 619, 30-7 (2007).
20. Garzon, R. et al. MicroRNA fingerprints during human megakaryocytopoiesis. *Proc Natl Acad Sci U S A* (2006).
21. Shingara, J. et al. An optimized isolation and labeling platform for accurate microRNA expression profiling. *Rna* (2005).
22. Calin, G.A. et al. Human microRNA genes are frequently located at fragile sites and genomic regions involved in cancers. *Proc Natl Acad Sci U S A* 101, 2999-3004 (2004).
23. Yang J, Z.F., Xu T, Deng H, Ge YY, Zhang C, Li J, Zhuang SM. Analysis of sequence variations in 59 microRNAs in hepatocellular carcinomas. *Mutat Res* (2007).
24. Lagos-Quintana, M. et al. Identification of tissue-specific microRNAs from mouse. *Curr Biol* 12, 735-9 (2002).
25. Chang, J. et al. miR-122, a Mammalian Liver-Specific microRNA, is Processed from hcr mRNA and May Downregulate the High Affinity Cationic Amino Acid Transporter CAT-1. 1, 106 (2004).
26. Jopling, C.L., Yi, M., Lancaster, A.M., Lemon, S.M. & Sarnow, P. Modulation of hepatitis C virus RNA abundance by a liver-specific MicroRNA. *Science* 309, 1577-81 (2005).
27. Krek, A. et al. Combinatorial microRNA target predictions. *Nat Genet* (2005).
28. Lim, L.P. et al. Microarray analysis shows that some microRNAs downregulate large numbers of target mRNAs. *Nature* 433, 769-73 (2005).
29. Wang, X. & Wang, X. Systematic identification of microRNA functions by combining target prediction and expression profiling. *Nucleic Acids Res* 34, 1646-1652 (2006).
30. Conaco, C., Otto, S., Han, J.J. & Mandel, G. Reciprocal actions of REST and a microRNA promote neuronal identity. *Proc Natl Acad Sci U S A* (2006).
31. Kutay, H. et al. Downregulation of miR-122 in the rodent and human hepatocellular carcinomas. *J Cell Biochem* (2006).
32. Kiriakidou, M. et al. A combined computational-experimental approach predicts human microRNA targets. *Genes Dev* 18, 1165-78 (2004).
33. Meng, F. et al. Involvement of human micro-RNA in growth and response to chemotherapy in human cholangiocarcinoma cell lines. *Gastroenterology* 130, 2113-29 (2006).
34. Gaur, A. et al. Characterization of MicroRNA Expression Levels and Their Biological Correlates in Human Cancer Cell Lines. *Cancer Res* 67, 2456-68 (2007).

35. Brown, B.D., Venneri, M.A., Zingale, A., Sergi, L.S. & Naldini, L. Endogenous microRNA regulation suppresses transgene expression in hematopoietic lineages and enables stable gene transfer. *Nat Med* (2006).
36. Bandres, E. et al. Identification by Real-time PCR of 13 mature microRNAs differentially expressed in colorectal cancer and non-tumoral tissues. *Mol Cancer* 5, 29 (2006).
37. Sonkoly, E. et al. MicroRNAs: Novel Regulators Involved in the Pathogenesis of Psoriasis? *PLoS ONE* 2, e610 (2007).
38. Lehmann, U. et al. Epigenetic inactivation of microRNA gene hsa-mir-9-1 in human breast cancer. *J Pathol* (2007).
39. Li, Q.J. et al. miR-181a is an intrinsic modulator of T cell sensitivity and selection. *Cell* 129, 147-61 (2007).
40. Chen, C.Z., Li, L., Lodish, H.F. & Bartel, D.P. MicroRNAs modulate hematopoietic lineage differentiation. *Science* 303, 83-6 (2004).
41. Pekarsky, Y. et al. Tcl1 expression in chronic lymphocytic leukemia is regulated by miR-29 and miR-181. *Cancer Res* 66, 11590-3 (2006).
42. Naguibneva, I. et al. The microRNA miR-181 targets the homeobox protein Hox-A11 during mammalian myoblast differentiation. *Nat Cell Biol* (2006).
43. Ciafre, S.A. et al. Extensive modulation of a set of microRNAs in primary glioblastoma. *Biochem Biophys Res Commun* 334, 1351-8 (2005).
44. Garzon, R. et al. MicroRNA gene expression during retinoic acid-induced differentiation of human acute promyelocytic leukemia. *Oncogene* (2007).
45. Volinia, S. et al. A microRNA expression signature of human solid tumors defines cancer gene targets. *Proc Natl Acad Sci U S A* (2006).
46. Hsu, P.W. et al. miRNAMap: genomic maps of microRNA genes and their target genes in mammalian genomes. *Nucleic Acids Res* 34, D135-9 (2006).
47. Kato et al. MicroRNA-192 in diabetic kidney glomeruli and its function in TGF-beta-induced collagen expression via inhibition of E-box repressors. (2007).
48. Iorio, M.V. et al. MicroRNA Signatures in Human Ovarian Cancer. *Cancer Res* 67, 8699-8707 (2007).
49. Hurteau, G.J., Carlson, J.A., Spivack, S.D. & Brock, G.J. Overexpression of the MicroRNA hsa-miR-200c Leads to Reduced Expression of Transcription Factor 8 and Increased Expression of E-Cadherin. *Cancer Res* 67, 7972-6 (2007).
50. Tran, N. et al. MicroRNA expression profiles in head and neck cancer cell lines. *Biochem Biophys Res Commun* 358, 12-17 (2007).
51. Martinez, I. et al. Human papillomavirus type 16 reduces the expression of microRNA-218 in cervical carcinoma cells. *Oncogene* (2007).
52. Lum, A.M. et al. Retroviral activation of the mir-106a microRNA cistron in T lymphoma. *Retrovirology* 4, 5 (2007).
53. Voorhoeve, P.M. et al. A genetic screen implicates miRNA-372 and miRNA-373 as oncogenes in testicular germ cell tumors. *Cell* 124, 1169-81 (2006).
54. Poy, M.N. et al. A pancreatic islet-specific microRNA regulates insulin secretion. *Nature* 432, 226-30 (2004).
55. Huang, J. et al. Cellular microRNAs contribute to HIV-1 latency in resting primary CD4(+) T lymphocytes. *Nat Med* 13, 1241-7 (2007).